

Evaluation of Mean Recurrence Intervals of Wind Effects for Tall Building Design

Rene D. Gabbai¹ and Emil Simiu²

¹ Assistant Professor, The Catholic University of America, Washington, DC 20064

Rene.Gabbai@GenesisOilandGas.Com

² NIST Fellow, National Institute of Standards and Technology, Gaithersburg, MD 20899

emil.simiu@nist.gov

Abstract

In current practice MRIs of wind effects specified for the Strength Design (SD) of tall, flexible buildings by the wind tunnel method are based on estimates of total uncertainties in the wind effects that do not account in a building-specific manner for the contribution of uncertainties in the dynamic parameters (natural frequencies and damping ratios). The purpose of this work is to present a procedure for assessing the acceptability of this practice. The procedure accounts for the probability distributions of total uncertainties in basic wind effects, defined herein as wind effects corresponding to MRIs of the order of 50 or 100 years. The total uncertainties are estimated for two cases. For Case 1 only uncertainties in the wind loading are taken into account. For Case 2 uncertainties in both the wind loading *and* the dynamic parameters are considered. Cumulative distribution functions of the total uncertainties in the basic wind effects are determined by Monte Carlo simulation. To assure risk consistency it is required that

the MRIs of wind effects considered for SD correspond in both cases to the same upper confidence bound of the basic wind effects. Using as an example a 305 m tall symmetrical steel building with coincident elastic and mass centers it was found that, under a specified set of assumptions on the uncertainties in the wind loading and the dynamic parameters, the requisite MRIs are larger for Case 2 than for Case 1 by at most 80 %. To these increases there corresponded wind effects considered for SD larger for Case 2 than for Case 1 by at most 6 %. The methodology presented in the paper is also applicable to buildings with non-coincident elastic and mass centers,

Keywords: Confidence bounds; flexible buildings; mean recurrence interval; risk consistency; structural dynamics; strength design; structural reliability; tall buildings; uncertainties; wind effects.

Introduction

Mean recurrence intervals (MRIs) specified by codes and standards for wind effects associated with Allowable Stress Design have typically been of the order of 50 to 100 years. We refer to these wind effects as basic wind effects, and denote their MRIs by \bar{N}_1 . For wind effects considered in Strength Design (SD) the specified MRIs are typically of the order of 500 to

2000 years. We denote these MRIs by \bar{N}_2 . For example, some codes specify for certain applications $\bar{N}_1 = 50$ years or $\bar{N}_2 = 500$ years.

Historically, the wind effect with MRI \bar{N}_2 has been determined as the product of the wind effect with MRI \bar{N}_1 by a wind load factor larger than unity reflecting the total uncertainty in the basic wind effect (see, e.g., Ellingwood et al., 1980). The wind load factor is an increasing function of the total uncertainty in the wind effect. Hence so is the MRI \bar{N}_2 . Note that the ASCE 7-10 Standard (ASCE 2010) has introduced the following change. Wind effects used for SD are no longer obtained, as in earlier versions of the Standard, through multiplication of wind effects with MRI \bar{N}_1 by a wind load factor larger than unity. Rather, the wind load factor implicit in the ASCE 7-10 Standard is unity (i.e., it does not reflect uncertainties in the estimation of wind effects), and the wind effects used for SD have specified MRIs \bar{N}_2 approximately equal to the MRIs of the wind effects for SD implicit in those earlier versions. The wind effects specified for SD in the ASCE 7-10 Standard thus account for approximately the same uncertainties that are inherent in the wind load factors specified in the Standard's earlier versions."

Uncertainties in the dynamic parameters (natural frequencies and damping ratios) contribute to increasing the total uncertainty in the wind effects. Therefore, accounting for the uncertainties in the dynamic parameters will result in an increase in the value of the MRI \bar{N}_2

with respect to the case in which these uncertainties are not accounted for. That increase is not accounted for in the ASCE 7-10 Standard. The purpose of this study is to present a procedure for estimating the degree to which that increase may be significant from a structural design viewpoint.

Fundamentally, insofar as it based on uncertainty calculations, our approach is similar to the approach used by Ellingwood et al. (1980, p. 117) for application to structures designed by so-called analytical methods, that is, to structures that do not experience von Kármán vorticity effects and are therefore assumed to experience only along-wind response. In contrast, the procedure presented in this work is applicable to tall, flexible buildings designed by the wind tunnel method, and therefore accounts for simultaneous wind effects due to motions along the two principal axes of the buildings and in torsion. In addition, our procedure is consistent with the fact that wind effects on flexible structures are commensurate with wind speeds raised to powers typically larger than two, whereas the procedure developed for use in analytical methods only considers responses proportional to wind speeds raised to the second power. Finally, our procedure accounts rigorously for wind directionality effects, rather than using a blanket directionality factor considered to be appropriate for structures designed by analytical methods. The implementation of our approach is now possible because current computational capabilities are far greater than those available three decades ago.

The procedure presented in this work entails the use of Monte Carlo simulations performed for two cases. For Case 1 the total uncertainties in the basic wind effects are associated with the wind loading only. For Case 2 they are associated with both the wind loading *and* the dynamic parameters. The simulations produce estimates of the cumulative distribution functions of the total uncertainties in the basic wind effects. We require that risks inherent in SD design be equal for Case 1 and Case 2. For this to be the case \bar{N}_2 must correspond in both cases to the same upper confidence bound of the wind effect with specified MRI \bar{N}_1 . As is shown in the paper, this requirement defines the value of the wind effect to be used for SD in Case 2. A non-parametric statistical approach is then employed to estimate the corresponding value of \bar{N}_2 . Using as an example a 305 m tall steel building it is found, under a specified set of assumptions regarding the distributions of the individual uncertainties being considered, that the requisite MRI \bar{N}_2 is larger for Case 2 than for Case 1 by at most 80 %, and that to these increases there correspond wind effects considered for SD larger for Case 2 than for Case 1 by at most 6 %. This suggests that, to the extent that the assumptions on uncertainties used in our example are warranted, current practice pertaining to the MRI \bar{N}_2 of wind effects considered for the SD of tall buildings is acceptable for buildings similar to the building considered in this paper. However, the difference can be larger for buildings with

irregular shapes and non-coincident mass and elastic centers, for which the dynamic analysis is described, for example, in Simiu (2011, Section 14.4).

In the following sections we discuss the uncertainties characterizing the wind effects, describe the proposed evaluation procedure, describe the Monte Carlo procedure used to construct the probability distributions of the total uncertainties in the basic wind effects, and provide an example of its application.

Uncertainties

The uncertainties associated with the wind loading consist of the micrometeorological, aerodynamic, and wind climatological uncertainties, while those associated with the dynamic parameters pertain to the modal periods and damping ratios. We denote by a , b , and c , respectively, the random variables reflecting uncertainties in the wind tunnel measurements of the pressures, in the conversion of 3-s (or 1 min) speeds over open terrain to hourly (or 10-min) mean speeds at the top of the building, and in the estimation of extreme wind speeds. The uncertainties in the damping and natural periods are characterized by random variables denoted by d and T , respectively.

The properties of the probabilistic distributions used in this work to model the uncertainties a , b , c , d and T are given in Table 1. To gain an insight into the effect of the choice of damping distribution on the results being sought, two distributions are considered for the modal

damping ratios, the lognormal distribution and the truncated normal distribution. The lognormal distribution has been previously considered by other researchers (Bashor and Kareem, 2009). Unlike the truncated normal distribution, it is positively skewed.

The distributions of Table 1 are subjective, that is, they are based on judgment and are used in this paper for illustrative purposes. Truncated distributions were assumed for the normal distributions because it would be unreasonable to believe that, for example, the error in the pressure measurement could be infinitely large or exceed a reasonable finite amount. However, different distributions, judged to be more realistic and possibly more unfavorable (longer-tailed), may be used should practitioners or Standard committees judge this necessary.

Evaluation Procedure

Denote by $F(\bar{N}_1)$ the \bar{N}_1 -year estimate of the wind effect F of interest. In the presence of the uncertainties described in the previous section, $F(\bar{N}_1)$ is a random variable that can be described by the cumulative distribution function $P[F(\bar{N}_1)]$. The \bar{N}_1 -year point estimate of that random variable is denoted by $\text{loc}[F(\bar{N}_1)]$, where “loc” designates “location.” In our calculations we chose the median as a measure of location. This choice is convenient but not obligatory; the mean could be chosen instead. As was mentioned earlier, \bar{N}_1 is typically of the order of 50 to 100 years, its value being deemed on the basis of experience to be adequate for

certain classes of structures and certain wind climates. For SD it is necessary to specify a point estimate of the \bar{N}_2 -year design wind effect, $\text{loc}[F(\bar{N}_2)]$.

Calculations and committee decisions based on a set of typical uncertainties with respect to micrometeorological, climatological, and aerodynamic parameters have led to the specification in various standards of the MRI \bar{N}_2 . As was pointed out earlier, those calculations did not cover in detail the case of tall, flexible structures. Rather, they were appropriate for typical buildings designed by so-called analytical methods, rather than on the basis of wind tunnel tests.

We consider the MRI \bar{N}_1 specified for all structures belonging to a given risk category in a given wind climate, and assume that the MRI \bar{N}_2 (henceforth denoted by \bar{N}_{2r}) is based on uncertainties in the wind loading only, without accounting for uncertainties in the dynamic parameters. We calculate the counterpart of the MRI \bar{N}_{2r} (henceforth denoted by \bar{N}_{2f}) that accounts, in addition to the uncertainties in the wind loading, for the uncertainties in the flexible structure's dynamic parameters. Thus, the subscripts "*r*" and "*f*" indicate, respectively, that the response corresponds to the total uncertainties due to uncertainties in the wind loading only and to larger total knowledge uncertainties due to uncertainties in the wind loading *and* the dynamic parameters. The subscripts have the same meaning when applied to the respective wind effects *F*.

The calculation of \bar{N}_{2f} is performed as follows:

1. Obtain the cumulative probability distributions $P[F_r(\bar{N}_1)]$ and $P[F_f(\bar{N}_1)]$ by Monte Carlo simulations, as indicated in the next section of the paper. Determine the point estimates inherent in those distributions, that is, $\text{loc}[F_r(\bar{N}_1)]$ and $\text{loc}[F_f(\bar{N}_1)]$.
2. For the structure with no uncertainties in the dynamic parameters, determine the percentile p of the distribution $P[F_r(\bar{N}_1)]$ for which the wind effect, denoted by $[F_r(\bar{N}_1)]_p$, is equal to the point estimate, $\text{loc}[F_r(\bar{N}_{2r})]$, of the wind effect F_r with the specified MRI \bar{N}_{2r} (see Fig. 1). As indicated earlier, depending upon the standard being considered, \bar{N}_{2r} as specified in various codes and standards is typically of the order of 500 to 2000 years.
3. To achieve risk consistency, the wind effect for SD of the structure assumed to have no uncertainties in the dynamic parameters must be equal to $[F_f(\bar{N}_1)]_p$, that is, to the value of $F_f(\bar{N}_1)$ corresponding in the distribution $P[F_f(\bar{N}_1)]$ to the percentile p (or, if the building owner or the building official so chooses, to a percentile $p_f \geq p$). The mean recurrence interval \bar{N}_{2f} of the wind effect considered for SD is then obtained from the equality $\text{loc}[F_f(\bar{N}_{2f})] = [F_f(\bar{N}_1)]_p$.

The probability distributions $P[F_r(\bar{N}_1)]$ and $P[F_f(\bar{N}_1)]$ are determined by using assumed distributions of the uncertainties being considered. Those distributions are not known.

However, they can be assumed on the basis of judgment and experience, as was done in Table

1. Once the distributions of the uncertainties are assumed, $P[F_r(\bar{N}_1)]$ and $P[F_f(\bar{N}_1)]$ are obtained from Monte Carlo simulations. The following section is devoted to a description of the Monte Carlo simulations.

Monte Carlo Simulations

The response of a tall building to wind loading can be obtained by using frequency-domain or time-domain methods. Frequency-domain methods transform differential equations into algebraic equations. They have been developed and adopted in earlier decades owing in part to computational difficulties experienced in the numerical solution of the systems of differential equations governing building motions. The development of powerful computational capabilities has removed these difficulties. In addition, measurement methods have been developed in the past two decades that allow simultaneous measurements of pressure time histories at large numbers of points on the external surface of laboratory models. From such measurements it is possible to record simultaneous time histories of aerodynamic pressures at these points. These time histories form aerodynamic databases that characterize the building's aerodynamic behavior. The development of the time-domain methodology and software for determining the response of tall buildings in the time domain, is documented, e.g., in Venanzi, Fritz, and Simiu (2005), Simiu, Gabbai, and Fritz (2008), Spence (2009), Yeo (2011), Yeo and

Simiu (2011), and Simiu (2011). We briefly describe this methodology, described in detail in Spence (2009) and Yeo and Simiu (2011).

The building response of interest with a specified MRI is determined in several steps. (Examples of responses include the top floor acceleration at a corner of the top floor, and the demand-to-capacity index (DCI) for any given cross section of any given member; the DCI represents the left-hand side of the interaction equation for the design of structural members, see section “Example” in this paper for details.) First, a response database is obtained for each of F_l responses, $l = 1, 2, \dots, n$. Each response F_l is calculated separately for a sufficient number of wind speeds (e.g., 20, 30, ..., 80 m/s) blowing from a sufficient number of directions (e.g., N, N-NE, NE, ..., N-NW). The response database is a property of the structure independent of the wind climate, and provides information on the response induced by wind velocities with various speeds and directions (Simiu, 2011, p. 275). The separate calculation of the responses for a number of wind speeds is necessary because, as was mentioned earlier, unlike for the case of rigid structures dynamic effects result in wind effects no longer proportional to the square of the wind speeds.

The second step consists of the development of a sufficiently large matrix $[v]$ of directional wind speeds with standard micrometeorological features (i.e., standard averaging time, standard height above terrain with standard open exposure). This matrix constitutes a wind climatological database characterizing the wind climate of the region around the

building. The element v_{ij} of the matrix $[v]$ denotes the wind speed from direction j in wind event i . For hurricane-prone coastal areas in the U.S., such matrices, developed by simulation from basic climatological data (e.g., pressure defect, radius of maximum wind speeds, translation speed and direction), see, e.g., Chapter 3 in Simiu and Scanlan (1996), are available in the public domain on www.nist.gov/wind. The number of simulated events contained in each matrix is 999. Similar matrices are available commercially. For non-hurricane-regions, matrices $[v]$ can be developed by simulation from measured wind speed data as shown, for example, in Grigoriu (2009).

Using information from the response database corresponding to any desired wind effect F_l , the matrix $[v]$ is transformed into a set of n matrices $[F_l]$ ($l = 1, 2, \dots, n$) representing the wind effect $F_{l,ij}$ induced by the wind speed v_{ij} . However, for design purposes only the largest of the directional wind effects induced by a given wind event i , that is, only $\max_j (F_{l,ij})$, is of interest. By eliminating all elements of the matrix except the elements $\max_j (F_{l,ij})$ for all wind events i , a vector $\{F_{l,i}\}$ is formed that, after rank-ordering, can be used for the non-parametric estimation of the response F_l with any specified MRI (see, e.g., Simiu, 2011, p. 150 for details). This requires that the number of lines of the matrix $[v]$ be sufficiently large. For example, if the requisite MRI is 1350 years and the mean rate of arrival of the hurricane wind events is 0.56/year, as is the case for Miami, then the wind speeds matrix must contain a minimum number of $1350 \times 0.56 = 756$ events. The availability of a larger number of events

will improve the precision of the estimates. For measured wind speed events in extratropical storms the mean rate of arrival of the wind events, denoted by μ , is equal to or exceeds unity. The smallest requisite number of simulated events is, similarly, $\text{MRI} \times \mu$. For example, for a 500-year MRI and $\mu = 2/\text{year}$, that number is 1000.

Monte Carlo simulations of the responses involve the methodical repetition of these steps a large number of times, with different values of a , b , c , T , d , obtained randomly from the probability distribution of those variates, being used each time. In the Monte Carlo procedure each of the realizations of the variate a multiplies the measured pressure coefficients, while each of the realizations of the variates b and c multiplies the matrix $[v]$. This simple Monte Carlo simulation yields a reasonable approximation of the probability distribution of the basic wind effect being considered.

Example

To illustrate the calibration procedure outlined above, a 305 m tall, 74-story steel building is analyzed. As shown in Figure 2, structural members of the building consist of columns and beams. Slabs are not included in the analysis. Our calculations are not specifically tied to a specific set of standard provisions, and are only aimed to illustrate our procedure.

The mean modal damping ratios are assumed to be 1.5 % in all three modes considered (Table 1). Natural frequencies of vibration (Table 1) and mode shapes were calculated by

modal analysis using a finite element analysis program. Dynamic analyses of the building were performed by using wind loads corresponding to wind speeds of 20 m/s to 80 m/s in increments of 10 m/s, using the directional pressure data obtained from wind tunnel tests for suburban terrain exposure. The wind tunnel tests were performed at the Inter-University Research Center on Building Aerodynamics and Wind Engineering (CRIACIV-DIC) Boundary Layer Wind Tunnel in Prato, Italy. Note that for buildings sensitive to aeroelastic phenomena, synchronous pressures must be measured on an aeroelastic model under a range of wind speeds and directions for which aeroelastic responses occur (Diana et al. 2009). However, in this study aeroelastic effects are assumed not to be present.

For convenience the climatological database used in the study was chosen to be a dataset of 999 simulated hurricanes with wind speeds for 16 directions north of Miami, Florida (Milepost 1500), and was obtained from www.nist.gov/wind. This set was used because it is available in the public domain; we had no access to commercially available hurricane wind speed data. The angles indicating those directions are from 22.5° to 360° clockwise from the North in 22.5° increments. In this study, the orientation angle of the building is 0° from the North. Suburban terrain exposure is assumed in all directions.

Monte Carlo simulations were performed for two different cases: the uncertainties in the building response pertain to the wind loading only (Case 1); and the uncertainties pertain to characteristics of both the wind loading and the dynamic properties (Case 2). In Case 1,

randomly selected values of the variable a and of the variables b, c multiply the pressure time series and wind speed data from the climatological database, respectively, while in Case 2, in addition to the set of random variables a, b, c , randomly selected values of the variables d and T are used. $N = 5000$ samples (realizations) were generated from the distributions listed in Table 1.

For each realization, the software for determining wind effects “High-Rise Database-Assisted Design for Steel Structures” (HR_DAD_1.1) is called. The software, available at www.nist.gov/wind, has been described in detail by Spence (2009) and Yeo (2011). For each call to the program, the demand-to-capacity indexes corresponding to the 50, 100, 500, and 1350-year MRIs for the set of six corner columns shown in Figure 3 were obtained by considering the load combination

$$1.2D + L + 1.0W \quad (1)$$

In Eq. (1), D is the total dead load, L is the live load, and W is the wind load. Given the load combination of Eq. (1), the demand-to-capacity indexes (DCIs), denoted by $b_j^c(t)$, are calculated by using the interaction formulas specified by AISC (AISC 2005). For member j ,

$$\frac{P_j^c(t)}{\phi P_j} \geq 0.2: \quad B_j^c(t) = \frac{P_j^c(t)}{\phi P_j} + \frac{8}{9} \left(\frac{M_{jX}^c(t)}{\phi_b M_{jX}} + \frac{M_{jY}^c(t)}{\phi_b M_{jY}} \right) \leq 1 \quad (2)$$

$$\frac{P_j^c(t)}{\phi P_j} < 0.2: \quad B_j^f(t) = \frac{P_j^c(t)}{2\phi P_j} + \left(\frac{M_{jX}^c(t)}{\phi_b M_{jX}} + \frac{M_{jY}^c(t)}{\phi_b M_{jY}} \right) \leq 1 \quad (3)$$

where P_j , M_{jX} and M_{jY} are the nominal axial and flexural strengths (axes X and Y in the local coordinate system) of the member, ϕ and ϕ_b are the axial and flexural resistance factors, and the quantities in the numerators are the total axial load and bending moments due to the specified factored combination of Eq. (1) (hence the superscript c).

The wind effects being considered here are the contributions of the wind loading to the interaction equation based on Eq. (1). That is, while the load combination of Eq. (1) was used to determine the appropriate interaction equation, the values used in this study are the $B_j^c(t)$ calculated using only the load $1.0W$. The wind effect of interest for member j is then $F_j = \max_t [B_j^c(t)]$.

At the end of the Monte Carlo simulations, one can construct the empirical distribution functions $P[F(\bar{N}_1)]$ with \bar{N}_1 chosen to be 50 years or 100 years. It was verified that the number of samples ($N = 5000$) was adequate for the purposes of this paper, that is, it allowed the determination of the percentile p that must be the same for Cases 1 and 2, as indicated in the section "Evaluation Procedure." To the percentile p there corresponds the requisite value of the wind effect to be used for Strength Design in Case 2. The MRI corresponding to that value is estimated from the rank-ordered vector of wind effects obtained as indicated in the section "Monte Carlo Simulations."

Table 2 summarizes results for the case where the damping d is normally distributed, while Table 3 summarizes results for the case where the damping is lognormally distributed. It is seen that the MRIs are in all cases larger for Case 2, in which uncertainties in the dynamic parameters are taken into account, than in Case 1, in which those uncertainties are disregarded. As may be expected, the increase differs from member to member, given that each member experiences a different demand-to-capacity index under wind loads. The results differ little as functions of distribution for the damping d . For this particular example, and for the distributions assumed in the calculations, increases in the MRIs were less than 80 % in all cases. To these increases there corresponded wind effects considered for SD larger for Case 2 than for Case 1 by at most 6 %. These results suggest that, for this example, to the extent that the assumptions on uncertainties used in our example are warranted, current practice pertaining to the MRIs of wind effects considered for the SD of tall buildings is acceptable.

Conclusions

We presented a practical procedure that evaluates MRIs of design wind effects with respect to specified MRIs, with a view to assuring a reasonable degree of risk consistency for structures experiencing wind-induced dynamic response. We do so by accounting explicitly for uncertainties in the structure's dynamic parameters. The effect of those uncertainties depends on the structure being considered. We rely on the following implicit definition of risk

consistency: two structures are risk-consistent if they are designed for the same upper confidence bound of the probability distribution of the basic wind effect with a specified MRI (e.g., 50 years for some applications). This definition yields different MRIs for Strength Design, depending upon whether uncertainties in the dynamic parameters are, or are not, accounted for.

The procedure presented in this work was applied to a tall structure. The results of the calculations showed that, for wind effects considered for Strength Design, increases in the MRIs were less than 80 % in all cases, while increases in wind effects themselves were less than 6 %. This suggests that, for the example considered in the paper, and to the extent that the assumptions on uncertainties used in our example are warranted, current practice pertaining to wind effects considered for the SD of tall buildings is acceptable. Nevertheless, for some special structures, including structures with irregular shape in plan and non-coincident mass and elastic centers, it is prudent to use the procedure developed in this work or a similar procedure to assess the effect of uncertainties in the dynamic parameters.

Acknowledgements

The wind tunnel data developed at the CRIACIV-DIC Boundary Layer Wind Tunnel were kindly provided by Seymour Spence of the University of Perugia. Helpful comments by

Adam L. Pintar and DongHun Yeo, of the National Institute of Standards and Technology are acknowledged with thanks.

References

- AISC (2005). *Specification for Structural Steel Buildings*, American Institute of Steel Construction, Chicago, IL.
- ASCE (2010). *Minimum design loads for buildings and other structures*, American Society of Civil Engineers, Reston, VA.
- Bashor, R. and Kareem, A. (2009). "Load Factors for Dynamically Sensitive Structures." *11th Americas Conference on Wind Engineering*, San Juan, Puerto Rico.
- Diana, G., Giappino, S., Resta, F., Tomasini, G., and Zasso, A. (2009). "Motion effects on the aerodynamic forces for an oscillating tower through wind tunnel tests." *11th European & African Conference on Wind Engineering*, Florence, Italy, 53-56.
- Ellingwood, B., Galambos, T. V., MacGregor, J. G. and Cornell, C. A. (1980). *Development of a Probability Based Load Criterion for American National Standard A58*, NBS Special Publication 577, National Bureau of Standards, Washington, D.C.
- Grigoriu, M. (2009). *Algorithms for generating large sets of synthetic directional data for hurricane, thunderstorm, and synoptic winds*. NIST Technical Note 1626, National Institute of Standards and Technology, Gaithersburg, MD. (see www.nist.gov/wind).

Simiu, E. (2011). *Design of Buildings for Wind*, 2nd ed. Hoboken: Wiley.

Simiu, E., Gabbai, R. D., and Fritz, W. P. (2008). "Wind-induced tall building response: a time-domain approach." *Wind and Structures*, 11(6), 427-440.

Simiu, E., and Scanlan, R.H. (1996), *Wind Effects on Structures*, 3rd ed., New York: Wiley.

Spence, S. M. J. (2009). *High-rise database-assisted design 1.1 (HR_DAD_1.1): Concepts, software, and examples*. NIST Building Science Series 181, National Institute of Standards and Technology, Gaithersburg, MD. (see www.nist.gov/wind).

Venanzi, I., Fritz, W.P., and Simiu, E. (2005). "Structural Design for Wind of Tall Buildings with Non-Coincident Mass and Elastic Centers: A Database-Assisted Design Approach." *Proceedings of the 6th Asia-Pacific Conference on Wind Engineering* (C.-K. Choi, ed.), Seoul, Korea.

Yeo, D. (2010). *Database-Assisted Design of high-rise reinforced concrete structures for wind: Concepts, software, and application*. NIST Technical Note 1665, National Institute of Standards and Technology, Gaithersburg, MD (available on www.nist.gov/wind).

Yeo, D. and Simiu, E. (2011). "High-rise reinforced concrete structures: Database-Assisted Design for Wind." *Journal of Structural Engineering* (137) 1340-1349.

Notations

a = Random variable reflecting uncertainties in wind tunnel pressure measurements

ASD = Allowable Stress Design

b = Random variable reflecting uncertainties in conversion of 3-s (or 1-min) at 10 m
 over open terrain to hourly (or 10-min) speeds at the top of the building

$B_j^f(t)$ = Demand-to-capacity index for member j

c = Random variable reflecting uncertainties in the estimation of extreme wind speeds

CDF = Cumulative distribution function

d = Random variable reflecting uncertainties in the damping ratios

D = Dead load

DCI = Demand-to-capacity index

f = Index indicating factored loads

$F, F_l, F_{l,ij}, F_r, F_f$ = Wind effect, l -th wind effect being considered, l -th wind effect induced by
 wind speed v_{ij} , wind effect determined by not accounting for uncertainties in dynamic pa
 rameters, wind effect determined by accounting for uncertainties in dynamic parameters
 for uncertainties in dynamic parameters, respectively

L = Live load

n = Total number of wind effects being considered

loc = Location

M_{jX}, M_{jY} = Nominal flexural strengths about axis X and axis Y , of cross-section, respectively

MRI = Mean Recurrence Interval

N = Number of realizations in Monte Carlo simulations

\bar{N}_1 = MRI of basic wind effects

$\bar{N}_2, \bar{N}_{2r}, \bar{N}_{2f}$ = MRI of wind effects considered for SD, MRI of wind effects considered for

SD if dynamic uncertainties are not taken into account, MRI of wind effects considered for

SD if dynamic uncertainties are taken into account, respectively

p = Upper confidence bound

P = Probability distribution

P_j = Nominal axial strength

SD = Strength Design

T = Random variable reflecting uncertainties in the natural periods of vibration

v_{ij} = Wind speed from direction j in wind event i

W = Wind load

μ = Mean rate of arrival

ϕ, ϕ_b = Axial, flexural resistance factors, respectively

List of Tables

Table 1. Description of random variables

Table 2. Calibration results \bar{N}_{2f} for d truncated normal

Table 3. Calibration results \bar{N}_{2f} for d lognormal

Table 1. Description of random variables

Random Variable	Probability Density	Mean	COV (%)	[Lower, Upper] Limits
a	Truncated Normal	1	10	$[-3\sigma, 3\sigma]$
b	Truncated Normal	1	5	$[-3\sigma, 3\sigma]$
c	Truncated Normal	1	10	$[-3\sigma, 3\sigma]$
T	Truncated Normal	$-^a$	12.5	$[-2.5\sigma, 2.5\sigma]$
d	Truncated Normal	1.5 %	40	$[-1.5\sigma, 1.5\sigma]$
	Lognormal	1.5 %	40	$[0, \infty)$

^a 5.40 s in modes 1 and 2, and 3.10 s in mode 3 for the building described in the Example section.

Accepted Manuscript
 Not Copyedited

Table 2. MRIs \bar{N}_{2f} for d truncated normal

Member	$\bar{N}_1 = 50$ years	$\bar{N}_1 = 100$ years
	$\bar{N}_{2r} = 500$ years	$\bar{N}_{2r} = 1350$ years
10133	660	1680
10158	710	1700
10184	740	1740
11321	800	1530
11346	780	1520
11372	700	1640

Accepted Manuscript
 Not Copyedited

Table 3. MRIs \bar{N}_{2f} for d lognormal

Member ID	$\bar{N}_1 = 50$ years	$\bar{N}_1 = 100$ years
	$\bar{N}_{2r} = 500$ years	$\bar{N}_{2r} = 1350$ years
10133	690	1700
10158	720	1720
10184	760	1780
11321	900	1540
11346	900	1540
11372	740	1690

Accepted Manuscript
 Not Copyedited

List of Figures

Fig. 1. Schematic of calibration procedure

Fig. 2. Schematic view of the 74-story building

Fig. 3. Plan view of building with locations of selected members

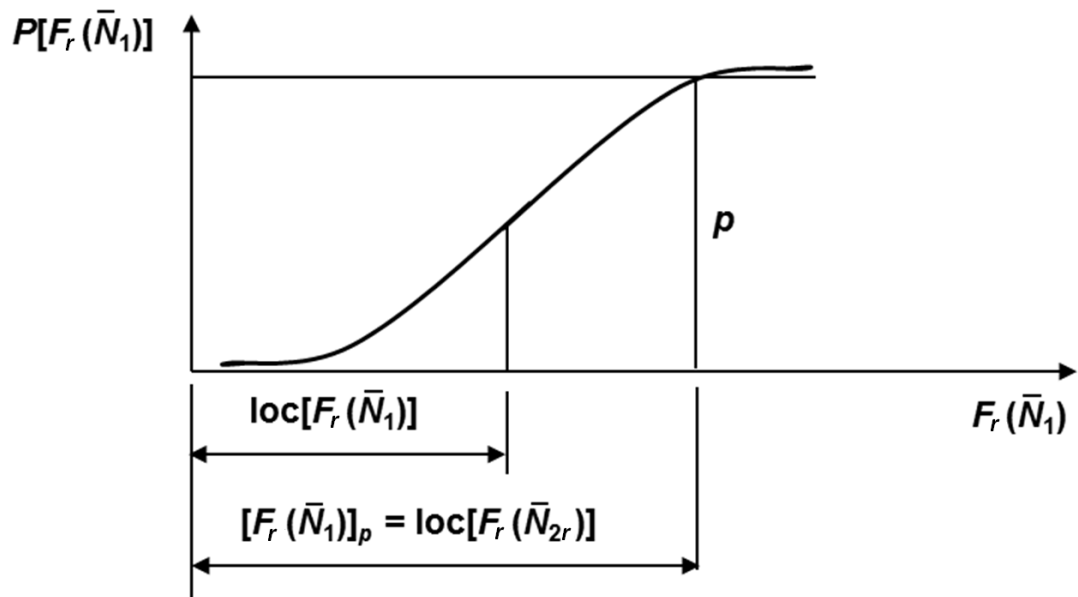


Fig. 1. Schematic of evaluation procedure

Accepted Manuscript
 Not Copyedited

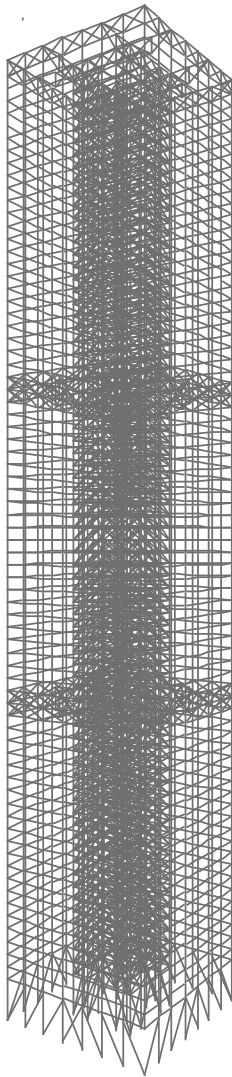


Fig. 1. Schematic view of the 74-story building

Accepted Manuscript
Not Copyedited

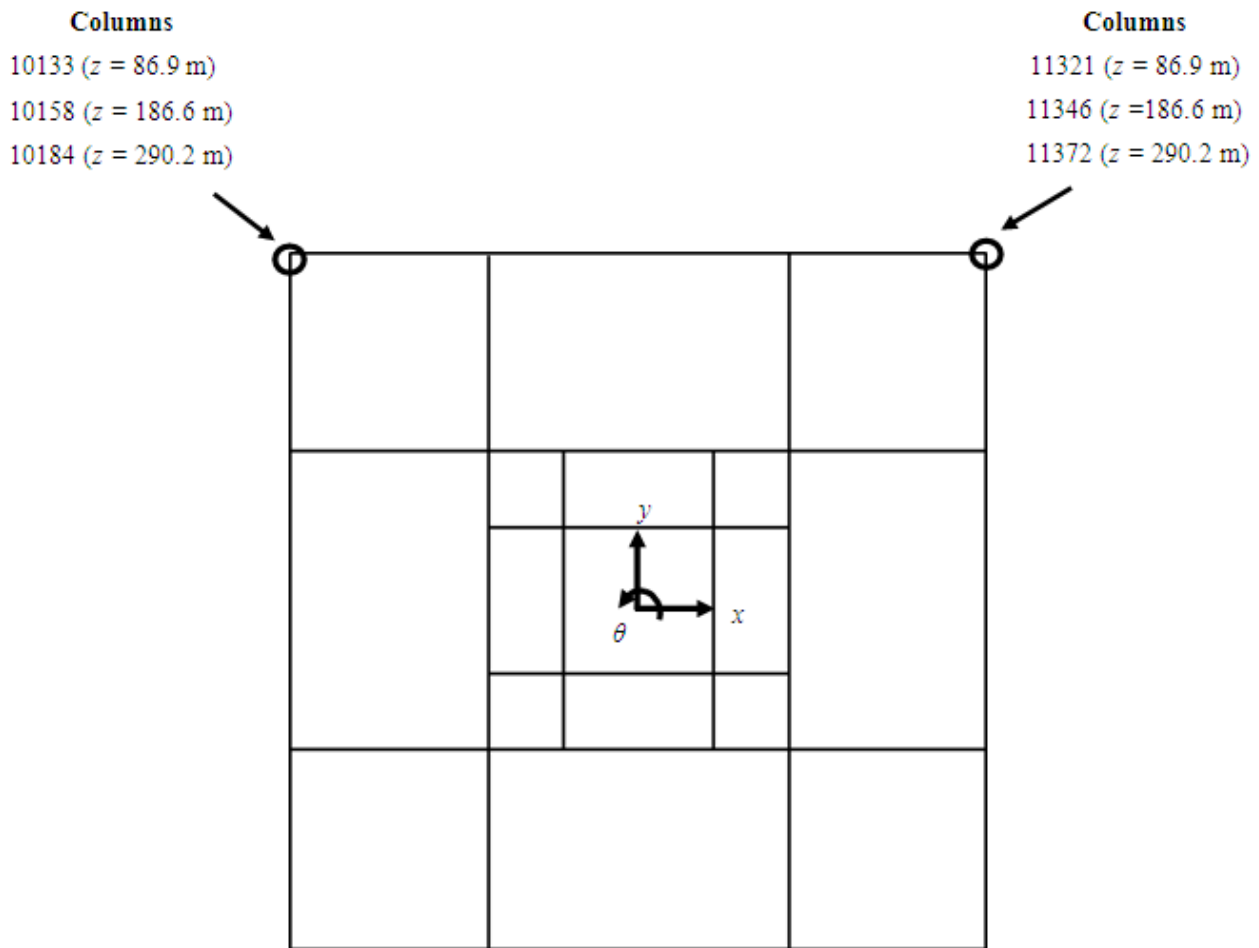


Fig. 3. Plan view of building with locations of selected members

Accepted Manuscript
 Not Copyedited